Growth–regime–controlled synthesis of $CdS–Bi_2S_3$ and Bi_2S_3 nanocrystals during the dissolution–recrystallization processes†

Xiaobo He, Lian Gao,* Songwang Yang and Jing Sun

Received 12th March 2010, Accepted 26th May 2010
DOI: 10.1039/c004208k

Inorganic composite nanocrystals have been widely investigated due to their novel properties and potential applications. However, to date, more effort is needed to suppress the homogeneous nucleation and self–growth of the second–component nanocrystals. In our work, we have introduced Bi^{3+} ions which can react with the CdS mother nanocrystals (NCs) during the dissolution processes of the mother NCs. Subsequently, the nanocrystals which recrystallize on the surfaces of the CdS mother nanocrystals are Bi_2S_3 nanocrystals rather than the mother ones due to the lower solubility of Bi_2S_3. Therefore, it is effective to avoid separation between the CdS mother nanocrystals and the second–component Bi_2S_3 nanocrystals. During this dissolution–recrystallization process, the growth regime can be facilely controlled from the thermodynamic control to the kinetic domination through adding more Bi^{3+} ions or changing the heating method from an oil bath to a microwave field. Consequently, the obtained $CdS–Bi_2S_3$ composite nanostructures can evolve from core–shell to tangentially–bonded structures in the oil bath, while tangentially–bonded $CdS–Bi_2S_3$ composite NCs and nest–shaped Bi_2S_3 NCs can be achieved in the microwave field.

1. Introduction

Inorganic nanocrystals (NCs) which possess extensive applications in biological imaging,[1] electronic devices,[2] and luminescence,[3] have attracted much attention in recent years. The integration of NCs with different properties into a single unit can advance the functions of NCs, Some inorganic composite NCs such as dumbbell–like nanoparticles (NPs),[4] match–like composite nanorods (NRs),[5] and core–shell quantum dots[6–8] have been created through two–step synthetic protocols in solution–phase processes. However, the drawback of the general routes is that much effort is needed to delicately suppress the homogeneous nucleation and self–growth of the second–component NCs.[4–9] Hence, it is attractive to develop more facile routes for the synthesis of composite NCs. In recent years, a method called ion exchange has been utilized to favor the growth of the secondary materials on the surfaces of the mother NCs without the separate growth in solution.[10,11] A series of composite NCs, including match–shaped $CdS–Cu_2S$ NRs,[12] $CdS–Ag_2S$ superlattice NRs,[13] and core–shell ZnS-ZnO composite NCs,[14] have been prepared through ion exchange. Furthermore, the galvanic replacement reaction can also be applied to synthesize composite NCs, such as Ag@AgAu metal core–shell NCs,[15] Pd–Au composite nanostructures,[16] and Pd–Ag nanoboxes.[17] Actually, it should be observed that the reactions for the formation of the second–component NCs at the interfaces involve the mother ones. In other words, the precursors of the second–component NCs should include the mother NCs and the other reactants, which can effectively prevent separation for both of them.

Interestingly, the dissolution–recrystallization mechanism can induce the conversion of the shapes of NCs from one to another during one–pot reactions. For example, Yang *et al.* have prepared triangular silver nanoplates transformed from nanospheres during the dissolution–recrystallization processes.[18] Xi *et al.* have fabricated a novel groovelike nanostructure of *t*–selenium on the basis of the dissolution–recrystallization mechanism, where the feeding of selenium atoms for the nanotubes arises from the diffusion on and/or near the surfaces of the microspheres.[19] In other words, dissolution–recrystallization processes can be controlled at the interfaces between the solid NCs and the solutions, which also can be utilized to synthesize the composite NCs and/or to obtain the novel nanostructures. In this paper, we intend to introduce a precursor which can react with the mother NCs during the dissolution processes of the mother NCs. Subsequently, the NCs which recrystallize on the surfaces of the mother NCs will be the second–component NCs rather than the mother ones due to the lower solubility of the secondary materials. As a result, the composite NCs will be prepared. CdS as a II–IV semiconductor has been widely investigated due to its potential applications in photocatalytic hydrogen production,[20] and solar cells,[21] while Bi_2S_3 is a thermoelectric material.[22] The combination of CdS and Bi_2S_3 in a single composite NC could hold possible applications in energy conversion. Therefore, in the practical synthesis, we selected flower–shaped CdS NCs and Bi^{3+} ions as the mother NCs and the precursor ions, respectively. Through controlling the feeding concentration of Bi^{3+} ions in an oil bath, a series of $CdS–Bi_2S_3$ composite NCs with different morphologies, such as the tangentially–bonded composite nanostructure, the core–shell and an intermediate composite nanostructure, have been obtained. Furthermore, tangentially–bonded $CdS–Bi_2S_3$ composite NCs and nest–shaped Bi_2S_3 NCs have also been prepared in a microwave field.

State key Laboratory of High Performance Ceramics and Superfine Microstructure, Shanghai Institute of Ceramics, Chinese Academy of Sciences, 1295 Dingxi Road, Shanghai, 200050, People's Republic of China. E-mail: liangaoc@online.sh.cn; Fax: +86 21 52413122; Tel: +86 21 52412718

† Electronic supplementary information (ESI) available: EDS spectrum collected from the *β*–NR shown in Fig. 2c; low–magnification TEM image of the sample S1; HRTEM image of the zone marked by a circle in Fig. 3d; photographs and the corresponding TEM images before and after heating treatment at 170 °C for 5 h without adding Bi^{3+} ions. See DOI: 10.1039/c004208k

2. Experimental

2.1 Synthesis of the CdS mother NCs

The CdS mother NCs were synthesized through procedures similar to our reported ones.[23] Typically, 0.5 mmol cadmium acetate hydrate and 4 mmol thiourea were dissolved in 50 mL deionized water. After stirring for 30 min, the mixed aqueous solution was transferred to a Teflon-lined stainless-steel autoclave with a capacity of 80 mL. The sealed autoclave was heated at 150 °C for 2 h in an oven. After reaction, the autoclave was cooled naturally. The yellowish colored precipitate was collected by centrifugation and washed by deionized water and anhydrous ethanol several times. The washed sample was dried at 60 °C for 6 h. ***Warning: Extra attention should be paid during the treatment of the hazardous cadmium acetate hydrate and CdS!***

2.2 Synthesis of CdS–Bi_2S_3 and Bi_2S_3 NCs

5 mg CdS mother NCs were dispersed into 50 g ethylene glycol (EG) by ultrasound for 30 min. 15 g yellowish dispersed liquid (containing ~0.01 mmol CdS) and 20 mL CTAB solution (5 mM in EG) were mixed and stirred for 15 min. Then Bi $(NO_3)_3 \cdot 5H_2O$ solution (5 mM in EG) was added dropwise at room temperature. The molar concentrations of the added Bi^{3+} ions before reaction are listed in Table 1. Thereafter, the reactions were carried out at 77 °C and 90 °C for 1.5 h with rapid stirring. Finally, the products were collected by centrifugation and washed with deionized water and anhydrous ethanol several times. To investigate the reactions in the extreme states, heat treatment without stirring was carried out in a household microwave oven (2.45 GHz, 800 W, 50 s). The other experimental parameters were kept constant except the concentration of the added Bi^{3+} ions listed in Table 1. It should be noted the mixed solutions were kept in an ice bath for 30 min before treatment in the microwave field.

2.3 Characterization

X-ray diffraction (XRD, D8 ADVANCE, Bruker AXS, Inc., Madison, WI, USA) measurements were performed to determine the phase compositions of the as–prepared NCs. Field emission transmission electron microscopy (FE–TEM, Model JEM–2100F, JEOL, Tokyo, Japan) was applied to observe the morphologies and microstructures of these NCs. The chemical compositions of the final products were collected using energy dispersive X-ray spectroscopy (EDS, Model ISIS, Oxford Microanalysis Group, High Wycombe, UK).

Table 1 Samples and the corresponding experimental parameters

Sample	Concentration of the added Bi^{3+} ions/mM	T/°C[a]
S1	0.28	77
S2	0.28	90
S3	0.09	90
S4	0.14	90
S5	0.19	90
S6	0.09	microwave
S7	0.28	microwave
S8	0.41	microwave

[a] The samples S1–S5 were heated in an oil bath, and the samples S6–S8 were prepared in a microwave field.

3. Results and discussion

Firstly, the reason for the use of the solvent EG should be pointed out. It is known that the precursor Bi $(NO_3)_3$ is easily hydrolyzed in aqueous solution as follows:

$$Bi(NO_3)_3 + H_2O \rightarrow BiONO_3\downarrow + 2HNO_3 \quad (1)$$

Obviously, the nitric acid can prevent the hydrolyzation of $Bi(NO_3)_3$. Is nitric acid solution suitable for carrying out the synthesis of the composite NCs? The answer is negative. The CdS NCs can be easily dissolved into the nitric acid solution before reaction with Bi^{3+} ions, especially under heat treatment. Furthermore, it is still difficult for $Bi(NO_3)_3$ to be dissolved in other organic solvents such as anhydrous ethanol, acetone, *N*,*N*-dimethylformamide and so on. Fortunately, on one hand, $Bi(NO_3)_3$ can be successfully dissolved in the solvent EG to form Bi^{3+} ions; on the other hand, the dissolution rate of the CdS NCs in EG is slower than in nitric acid solution. Therefore, EG was selected as the solvent for the synthesis of the CdS–Bi_2S_3 composite NCs and Bi_2S_3 NCs. The reaction between the precursor Bi^{3+} ions with the CdS NCs can be described as:

$$3CdS + 2Bi^{3+} \rightarrow Bi_2S_3 + 3Cd^{2+} \quad (2)$$

Fig. 1a shows the XRD pattern of the CdS mother NCs. All the diffraction peaks can be indexed to wurtzite–phased CdS (space group: $P6_3mc$, $a = 0.414$ nm, $c = 0.672$ nm), which are consistent with the standard diffraction card (JCPDS No. 41–1049). Obviously, the intensity of the (002) peak is more significant compared to that of the standard diffraction spectrum which is indicated by the vertical lines coupled with patterns in Fig. 1, implying the preferred growth of the CdS mother NCs along the [0001] direction. Fig. 1b shows the XRD pattern of the sample S1. Besides the diffraction peaks corresponding to the wurtzite CdS mother NCs, the other peaks can be assigned to orthorhombic Bi_2S_3 (JCPDS No. 17–0320), which demonstrates that the reaction (2) was carried out after adding Bi^{3+} ions to the EG suspension of the mother CdS NCs under heat treatment.

Fig. 2a shows the TEM image of the flower–shaped CdS mother NCs with an average diameter of 160 nm, which is similar to our previous results.[23] The SAED pattern in the inset of Fig. 2a shows the flower–shaped CdS mother NC is polycrystalline, which is composed

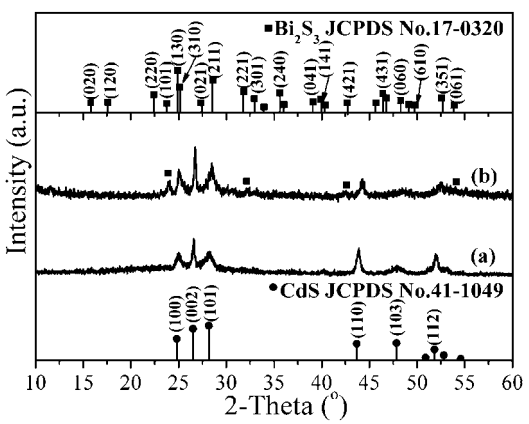

Fig. 1 XRD patterns before and after reaction (2): (a) the CdS mother NCs; (b) the sample S1.

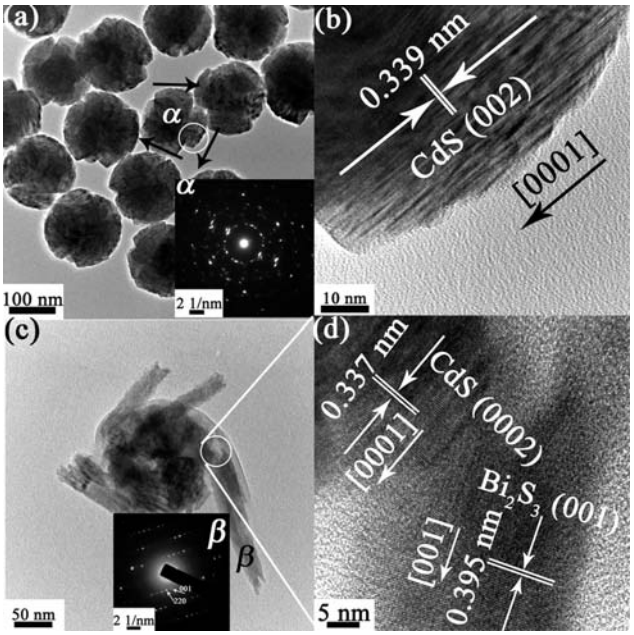

Fig. 2 Microstructure characterizations of the CdS mother NCs and the sample S1: (a) TEM image of the CdS mother NCs, the inset is the SAED pattern of an individual NC labeled by α; (b) HRTEM image of the zone in (a) marked by a circle; (c) TEM image of a typical tangentially–bonded CdS–Bi_2S_3 composite NC of the sample S1, the inset is the SAED pattern of the Bi_2S_3 NR labeled by β; (d) HRTEM image of the zone in (c) marked by a circle.

of several individual CdS NCs, namely building blocks. It is obvious that most of these plate–like building blocks grow preferentially. Fig. 2b presents the HRTEM image of the zone marked by a circle in Fig. 2a. The interplanar spacing along the preferred direction is about 0.339 nm, which can be indexed to the (0002) of wurtzite CdS. Hence, these CdS building blocks grow preferentially along the [0001] direction, which is also consistent with the XRD pattern shown in Fig. 1a. It is attractive that the preferred growth direction of these CdS building blocks is almost along the tangential direction of the entire mother NC, as shown in Fig. 2a by arrows.

As for the sample S1, a novel composite nanostructure, namely the tangentially–bonded composite nanostructure, was obtained after the reaction (2). As shown in Fig. 2c, several NRs are tangentially–bonded with the CdS mother NCs. According to the XRD pattern (Fig. 1b) and the EDS spectrum collected from the β–NR (Fig. S1†), these NRs with the average length of 140 nm and the diameter of 25 nm can be assigned to Bi_2S_3. The SAED pattern in the inset of Fig. 2c implies that the Bi_2S_3 NRs are single–crystalline, further confirmed by the corresponding HRTEM image in Fig. 2d. The HRTEM image in Fig. 2d shows the interface between the CdS mother NC and the Bi_2S_3 NR marked by a circle in Fig. 2c. The interplanar distance of ~0.337 nm corresponds to the (0002) of the wurtzite CdS (more concretely, the wurtzite CdS building block), while the interplanar distance of ~0.395 nm can be indexed to the (001) of the orthorhombic Bi_2S_3, which demonstrates that these Bi_2S_3 NRs prefer to grow along the [001] direction. It is noteworthy that the two preferentially growth directions for the CdS building blocks of the mother NCs and the Bi_2S_3 NRs, respectively, are nearly parallel. Therefore, it is understandable that the newly formed Bi_2S_3 NRs are arranged alongside the tangent direction of the entire mother NCs. Interestingly, there are no dissociative Bi_2S_3 NRs from the CdS mother NCs observed (Fig. S2†). In other words, the formed Bi_2S_3 NRs are all bonded with the CdS mother NCs through the interfaces shown in Fig. 2d. This implies that the reaction (2) is most probably carried out on the surfaces of the CdS mother NCs and naturally involves the mother NCs, which is similar to the effects of the ion exchange and galvanic replacement reactions in this sense.[12–17] On the other hand, as for the sample S1, the average diameter of the mother CdS NCs is decreased by about 20 nm after the reaction (2). Obviously, the consumed CdS are transferred to the Bi_2S_3 NRs. More accurately, the S^{2-} ions of the consumed CdS mother NCs are fed as the sulfur source for the formation of the Bi_2S_3 NRs. The morphology greatly differs before and after the reaction (2), which experiences the transformation from the nanoplates of the CdS building blocks for the mother NCs to the NRs of Bi_2S_3. In other words, although the second–component Bi_2S_3 NRs are almost conjoined with the mother NCs, they still have a degree of freedom for self growth. Noticeably, according to the effects of ion exchange reactions, there is less possibility for the secondary materials to develop totally different morphologies, leaving the mother NCs alone, especially when the mean size of the mother ones exceeds a critical value (generally 4~5 nm).[12–14] For example, Son *et al.* have reported that the initial nanostructures of CdS and CdTe can be preserved by Ag_2S and Ag_2Te respectively after the cation exchange reactions.[11] If the reaction (2) in our experiments followed the ion exchange mechanism, as a reasonable assumption, Bi_2S_3 would encircle the nanoplates of CdS building blocks to form tightly combined core–shell nanostructures.[11] However, as a matter of fact, the newly–formed Bi_2S_3 are endowed with the shapes of NRs. Even if the core–shell nanostructures are obtained in other experimental conditions which will be discussed in the following text, the Bi_2S_3 shells just loosely encapsulate the whole CdS mother NCs. Hence, there are few correlations between the formation of the tangentially–bonded CdS–Bi_2S_3 composite NCs and the ion exchange reactions. Fortunately, another process, namely dissolution–recrystallization, may dominate the feeding of S^{2-} ions and the free growth of the Bi_2S_3 NCs. Actually, some factors may affect the dissolution–recrystallization process, including temperature, the concentration of the added Bi^{3+} ions and the heating method.

As compared with the sample S1, the reaction temperature for the sample S2 was increased to 90 °C as listed in Table 1. Fig. 3a shows the TEM image of the sample S2. The tangentially–bonded CdS–Bi_2S_3 composite NCs still constitute the sample S2, where more Bi_2S_3 NRs have been achieved at the higher reaction temperature. Interestingly, the concentration of the added Bi^{3+} ions has a greater influence on the dissolution–recrystallization process than the reaction temperature does, and results in totally different composite nanostructures. As for the sample S3, 0.09 mM Bi^{3+} ions were employed. A core–shell nanostructure has been prepared, as shown in Fig. 3b. From the view of the HRTEM image of the zone marked by a circle, the inset of Fig. 3b indicates the average thickness of the Bi_2S_3 shells is about 3 nm. When more Bi^{3+} ions were introduced to the reaction solution (sample S4), obviously, thicker Bi_2S_3 shells were obtained (Fig. 3c). As shown in the inset of Fig. 3c, the thickness is increased to about 12 nm. It should be also noted that some of the Bi_2S_3 shells have disassociated from the mother NCs as arrowed in this inset. Some others have curled and expanded out from the central mother NCs as indicated by arrows in Fig. 3c and a circle in the inset,

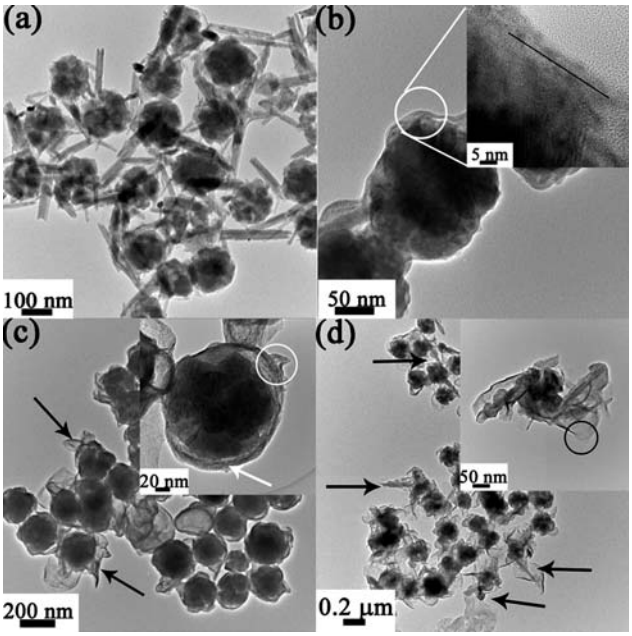

Fig. 3 TEM images of the other samples synthesized in an oil bath: (a) S2; (b) S3, the inset shows the HRTEM image of the zone marked by a circle; (c) S4, the inset is the TEM image of a typical core–shell CdS–Bi_2S_3 composite NC; (d) S5, the inset shows the TEM image of a typical intermediate CdS–Bi_2S_3 composite NC.

which implies the reaction interface may migrate outwards. According to the reported mechanism of the ion exchange reactions, the reaction interfaces continuously move inward to the mother NCs, rather than outward from the mother ones.[14,24] Hence, it is confirmed once more that the formation of CdS–Bi_2S_3 composite NCs following reaction (2) has little relationship with the ion exchange reactions, but is on intimate terms with the dissolution–recrystallization processes due to the outward diffusion of the dissolved ions from the mother NCs.[19] Furthermore, when the molar concentration of Bi^{3+} ions continued to increase to 0.19 mM, namely sample S5, the degree of curliness for almost all of the Bi_2S_3 shells has become more significant. It is also found that some curled Bi_2S_3 shells have been gradually twisted up to the NRs along the tangent direction of the mother NCs as indicated by arrows in Fig. 3d and viewed in the inset. Actually, these Bi_2S_3 shells are polycrystalline as shown in the HRTEM image of Fig.S3†, which is recorded from the zone marked by a circle in the inset of Fig. 3d. Hence, according to the microstructure analyses of the sample S1–S5, the composite nanostructure of the sample S5 can be considered as an intermediate one between the core–shell and the tangentially–bonded CdS–Bi_2S_3 composite NCs. From another perspective, the shape of the second–component Bi_2S_3 NCs can gradually evolve from the isotropic shells to the anisotropic NRs along with increasing concentration of Bi^{3+} ions, which, to the best of our knowledge, has been rarely reported.

When reaction (2) was carried out in a microwave field rather than in an oil bath, the situation was different. For the sample S6, the molar concentration of the added Bi^{3+} ions was 0.09 mM, the same as that of the sample S3. However, tangentially–bonded CdS–Bi_2S_3 composite NCs were achieved (Fig. 4a). When the concentration was increased to 0.28 mM, the nest–shaped NCs composed of NRs constituted the final sample S7 (Fig. 4b). According to the XRD

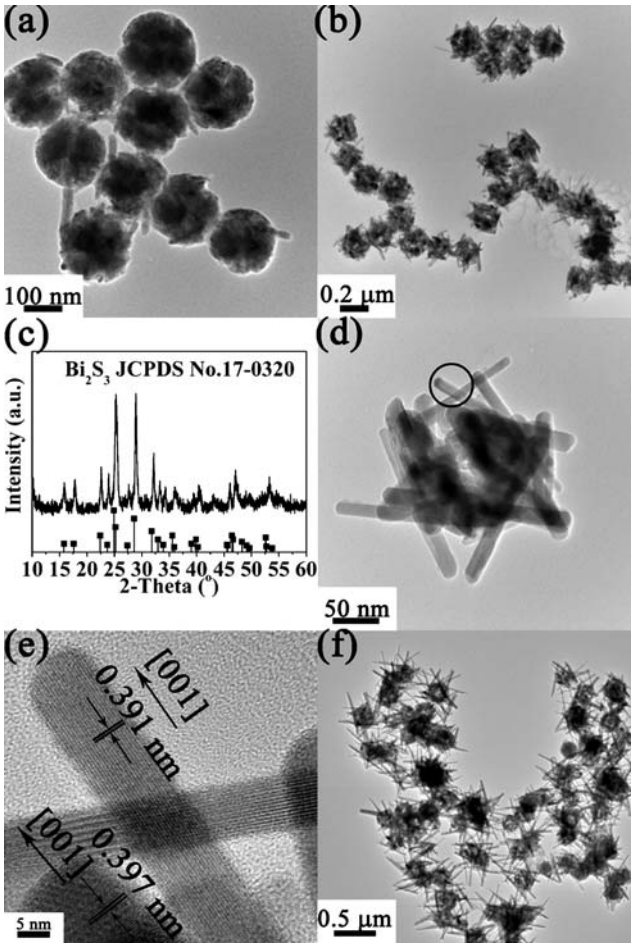

Fig. 4 (a) TEM image of sample S6; (b) TEM image of sample S7; (c) XRD pattern of the sample S7; (d) TEM image of a typical NC of the sample S7; (e) HRTEM image recorded from the zone indicated by a circle in (d); (f) TEM image of the sample S8.

pattern of the sample S7 (Fig. 4c), all diffraction peaks can be indexed to the orthorhombic Bi_2S_3 (JCPDS No. 17–0320), which demonstrates that the CdS mother NCs have been completely transformed to Bi_2S_3 NRs in the microwave field. Fig. 4d shows typically nest–shaped Bi_2S_3 NCs. The HRTEM image in Fig. 4e shows these single–crystalline Bi_2S_3 NRs in the nest–shaped NCs still grow preferentially along the [001] direction. When we continued to enhance the concentration of Bi^{3+} ions (the sample S8), obviously, the average aspect ratio of these Bi_2S_3 NRs is increased greatly by comparison with the sample S7, as shown in Fig. 4f.

On the basis of the above discussion, the formation of Bi_2S_3 is attributed to the dissolution–recrystallization process. The reaction (2) can be resolved as the two following reactions:

$$3CdS \rightleftarrows 3Cd^{2+} + 3S^{2-} \quad (3)$$

$$3S^{2-} + 2Bi^{3+} \rightleftarrows Bi_2S_3 \quad (4)$$

The reaction (3) indicates the dissolution of the CdS mother NCs, while the reaction (4) demonstrates the formation of Bi_2S_3 with the assistance of the feeding of the dissolved S^{2-} from mother NCs. Hence, the formation of Bi_2S_3 is controlled by the two reactions.

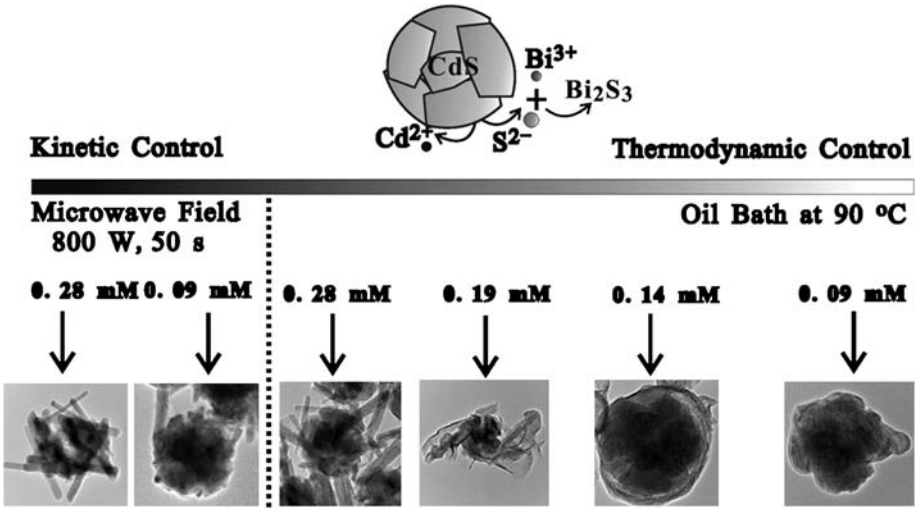

Fig. 5 Schematic diagram of the nanostructure evolution of the Bi_2S_3 and CdS–Bi_2S_3 NCs under different growth regimes during the dissolution–recrystallization processes. The concentration shown in this schematic diagram is indicated as the molar concentration of the added Bi^{3+} ions.

Obviously, when no Bi^{3+} ions are added, only reaction (3) works in theory. Interestingly, although the CdS mother NCs were heated at 170 °C for 5 h without adding Bi^{3+} ions, there were hardly any differences before and after this heating treatment, as shown in Fig. S4†. For example, the average diameter of the mother NCs is 160 nm before heat treatment, while the mean size is nearly retained after that. Therefore, actually, the dissolution of the CdS mother NCs is not visible without introducing Bi^{3+} ions. However, when the Bi^{3+} ions are fed in, the forward reaction of the reaction (4) begins to operate and Bi_2S_3 starts to occur, which further boosts the forward reaction of reaction (3) since the supply of S^{2-} ions results from the dissolution of the CdS mother NCs. In other words, the dissolution of the CdS mother NCs can be advanced by adding Bi^{3+} ions. As a matter of fact, the experimental results can also confirm the driving effect of Bi^{3+} ions on the dissolution of CdS. As shown in Fig. 2a and Fig. 2c, one can observe not only the existence of Bi_2S_3 NRs, but also the shrinking of CdS mother NCs. Thereby, it can be concluded that if more Bi^{3+} ions are imported from the outside, then more S^{2-} ions are provided from inside. Consequently, the flux of monomers for Bi_2S_3 can be controlled by the concentration of the added Bi^{3+} ions. Furthermore, as is known, the energy and mass transport is far faster in a microwave field than in an oil bath, where there are no thermal gradient effects.[3,25] And further, the selective dielectric heating of microwaves could excite the polar chalcogenide solids such as CdS.[26–29] Hence, in our experiments, the dissolution of the CdS mother NCs firstly driven by the added Bi^{3+} ions can be greatly further boosted by microwave heating, which can further promote the flux of monomers for the formation of Bi_2S_3 NCs.

When employing the same reaction temperature for the samples S2–S5 in an oil bath, although the high surface energy of the (001) planes of orthorhombic Bi_2S_3 and the selective adsorption of CTAB molecules can facilitate the growth of NRs,[30,31] the Bi_2S_3 NRs (sample S2) can be obtained only if the highest concentration of the added Bi^{3+} ions (~0.28 mM) is applied, as shown in Fig. 3. And as mentioned above, the higher flux of monomers for Bi_2S_3 can result from the higher concentration of Bi^{3+} ions. Further, according to the proposed growth mode for NRs by Peng *et al.*, the higher flux of monomers can result in the kinetic–controlled growth regime, which can favor one–dimensionally anisotropic growth for the NCs; otherwise, an isotropic growth regime controlled by thermodynamic factors would dominate.[32–34] Therefore, the formation of Bi_2S_3 NRs when the higher concentration of Bi^{3+} ions applied is probably ascribed to the kinetically favorable regime. In contrast, the growth of the 0D Bi_2S_3 nanoparticles (Fig. S3†) and the isotropic Bi_2S_3 shells (Fig. 3b and 3c) could be controlled thermodynamically. Namely, with the increase of the concentration of the added Bi^{3+} ions, the growth regime for Bi_2S_3 may undergo conversion from thermodynamic domination to kinetic control, which causes the evolution of composite nanostructures from the core–shell one, to an intermediate one, and finally to the tangentially–bonded composite one. Moreover, lower growth temperature can also facilitate the kinetically–controlled growth regime.[34,35] Hence, as for the sample S1, which is prepared by the same concentration of Bi^{3+} ions (~0.28 mM) with the sample S2, it is understandable to obtain Bi_2S_3 NRs and the tangentially–bonded composite nanostructure at the lower growth temperature. When heating in the microwave field, as discussed above, the high flux of monomers for Bi_2S_3 can be achieved. Consequently, the formation of Bi_2S_3 NRs controlled by a kinetic regime prevails at all times whatever the concentration of the added Bi^{3+} ions is applied, as shown in Fig. 4. Hence, according to the above discussion, the nanostructure evolution of these samples controlled by the growth regime during the dissolution–recrystallization process is proposed in Fig. 5.

4. Conclusions

In summary, we have introduced Bi^{3+} ions which can react with the CdS mother NCs during the dissolution processes of the mother NCs. Subsequently, the NCs which recrystallize on the surfaces of the CdS mother NCs are the Bi_2S_3 NCs rather than the mother ones. During this dissolution–recrystallization process, the growth regime can be facilely transformed from thermodynamic control to kinetic domination through adding more Bi^{3+} ions or changing the heating method from an oil bath to a microwave field. Consequently, the obtained CdS–Bi_2S_3 composite nanostructures can evolve from the core–shell ones to the tangentially–bonded ones in the oil bath, while

the tangentially–bonded CdS–Bi_2S_3 composite NCs and the nest–shaped Bi_2S_3 NCs can be readily prepared in the microwave field. Hence, the control of the nanoscale processes at the interfaces can promote rational protocols for the synthesis of composite NCs.

Acknowledgements

This work was supported by National Natural Science Foundation of China (Grant No. 50972157) and the Shanghai Nanotechnology Promotion Center (Grant No. 0852nm01900), respectively.

References

1 P. K. Jain, X. H. Huang, I. H. El-Sayed and M. A. El-Sayed, *Acc. Chem. Res.*, 2008, **41**, 1578.
2 H. L. Wang and L. M. Qi, *Adv. Funct. Mater.*, 2008, **18**, 1249.
3 A. B. Panda, G. Glaspell and M. S. El-Shall, *J. Phys. Chem. C*, 2007, **111**, 1861.
4 C. Wang, C. J. Xu, H. Zeng and S. H. Sun, *Adv. Mater.*, 2009, **21**, 3045.
5 T. Mokari, E. Rothenberg, I. Popov, R. Costi and U. Banin, *Science*, 2004, **304**, 1787.
6 D. C. Pan, Q. Wang, S. C. Jiang, X. L. Ji and L. J. An, *Adv. Mater.*, 2005, **17**, 176.
7 Y. Fu, T.-T. Han, H. Ågren, L. Lin, P. Chen, Y. Liu, G.-Q. Tang, J. Wu, Y. Yue and N. Dai, *Appl. Phys. Lett.*, 2007, **90**, 173102.
8 R. G. Xie, X. H. Zhong and T. Basché, *Adv. Mater.*, 2005, **17**, 2741.
9 P. Reiss, M. Protière and L. Li, *Small*, 2009, **5**, 154.
10 L. Dloczik and R. Könenkamp, *Nano Lett.*, 2003, **3**, 651.
11 D. H. Son, S. M. Hughes, Y. D. Yin and A. P. Alivisatos, *Science*, 2004, **306**, 1009.
12 B. Sadtler, D. O. Demchenko, H. M. Zheng, S. M. Hughes, M. G. Merkle, U. Dahmen, L.-W. Wang and A. P. Alivisatos, *J. Am. Chem. Soc.*, 2009, **131**, 5285.
13 R. D. Robinson, B. Sadtler, D. O. Demchenko, C. K. Erdonmez, L.-W. Wang and A. P. Alivisatos, *Science*, 2007, **317**, 355.
14 J. W. Park, H. M. Zheng, Y.-W. Jun and A. P. Alivisatos, *J. Am. Chem. Soc.*, 2009, **131**, 13943.
15 Q. B. Zhang, J. P. Xie, J. Y. Lee, J. X. Zhang and C. Boothroyd, *Small*, 2008, **4**, 1067.
16 X. W. Teng, Q. Wang, P. Liu, W. Q. Han, A. I. Frenkel, W. Wen, N. Marinkovic, J. C. Hanson and J. A. Rodriguez, *J. Am. Chem. Soc.*, 2008, **130**, 1093.
17 J. Y. Chen, B. Wiley, J. McLellan, Y. J. Xiong, Z. Y. Li and Y. N. Xia, *Nano Lett.*, 2005, **5**, 2058.
18 J. Yang, Q. B. Zhang, J. Y. Lee and H. P. Too, *J. Colloid Interface Sci.*, 2007, **308**, 157.
19 G. C. Xi, K. Xiong, Q. B. Zhao, R. Zhang, H. B. Zhang and Y. T. Qian, *Cryst. Growth Des.*, 2006, **6**, 577.
20 N. Z. Bao, L. M. Shen, T. Takata and K. Domen, *Chem. Mater.*, 2008, **20**, 110.
21 L. Wang, Y. S. Liu, X. Jiang, D. H. Qin and Y. Cao, *J. Phys. Chem. C*, 2007, **111**, 9538.
22 B. X. Chen, C. Uher, L. Iordanidis and M. G. Kanatzidis, *Chem. Mater.*, 1997, **9**, 1655.
23 X. B. He and L. Gao, *J. Phys. Chem. C*, 2009, **113**, 10981.
24 P. H. C. Camargo, Y. H. Lee, U. Jeong, Z. Q. Zou and Y. N. Xia, *Langmuir*, 2007, **23**, 2985.
25 A. B. Panda, G. Glaspell and M. S. El-Shall, *J. Am. Chem. Soc.*, 2006, **128**, 2790.
26 M. Q. Zhu, Z. Gu, J. B. Fan, X. B. Xu, J. Cui, J. H. Liu and F. Long, *Langmuir*, 2009, **25**, 10189.
27 K. J. Rao, B. Vaidhyanathan, M. ganguli and P. A. Ramakrishnan, *Chem. Mater.*, 1999, **11**, 882.
28 V. V. Antonov, S. V. Ivanov, V. P. Tsarev and V. N. Chupis, *Tech. Phys.*, 1998, **43**, 1358.
29 A. L. Washington II and G. F. Strouse, *Chem. Mater.*, 2009, **21**, 3586.
30 Y. Wang, J. Chen, P. Wang, L. Chen, Y. B. Chen, L. Wu and M., *J. Phys. Chem. C*, 2009, **113**, 16009.
31 Y. Jiang, Y. J. Zhu and Z. L. Xu, *Mater. Lett.*, 2006, **60**, 2294.
32 Z. A. Peng and X. G. Peng, *J. Am. Chem. Soc.*, 2001, **123**, 1389.
33 Y. W. Jun, J. S. Choi and J. Cheon, *Angew. Chem., Int. Ed.*, 2006, **45**, 3414.
34 Y. W. Jun, J.-H. Lee, J.-S. Choi and J. Cheon, *J. Phys. Chem. B*, 2005, **109**, 14795.
35 S.-M. Lee, Y.-W. Jun, S.-N. Cho and J. Cheon, *J. Am. Chem. Soc.*, 2002, **124**, 11244.

